

Statistical switching kinetics of ferroelectrics

This article has been downloaded from IOPscience. Please scroll down to see the full text article.

2009 J. Phys.: Condens. Matter 21 012207

(<http://iopscience.iop.org/0953-8984/21/1/012207>)

View [the table of contents for this issue](#), or go to the [journal homepage](#) for more

Download details:

IP Address: 129.252.86.83

The article was downloaded on 29/05/2010 at 16:53

Please note that [terms and conditions apply](#).

FAST TRACK COMMUNICATION

Statistical switching kinetics of ferroelectrics

X J Lou

Department of Materials Science and Engineering, National University of Singapore, 117574, Singapore

E-mail: msejx@nus.edu.sg

Received 9 October 2008, in final form 9 November 2008

Published 4 December 2008

Online at stacks.iop.org/JPhysCM/21/012207

Abstract

By assuming a more realistic nucleation and polarization reversal scenario we build a statistical switching model for polycrystalline ferroelectrics, which is different from both the Kolmogorov–Avrami–Ishibashi (KAI) model and the nucleation-limited-switching model.

After incorporating a time-dependent depolarization field, this model gives a good explanation of the retardation behavior in polycrystalline thin films at medium or low fields, which cannot be described using the traditional KAI model. This model predicts $n = 1$ for polycrystalline thin films at high fields or ceramic bulks in the *ideal* case, in good agreement with the experimental data previously published.

(Some figures in this article are in colour only in the electronic version)

1. Introduction

Polarization switching in ferroelectric materials has been intensively investigated both experimentally and theoretically for a few decades, since the first work was done by Merz in 1950s [1]. The traditional model used to describe the switching kinetics of ferroelectrics is the Kolmogorov–Avrami–Ishibashi (KAI) model [2–4], based on the classical theory of Kolmogorov [5] and Avrami [6]. For a fully poled ferroelectric capacitor driven by an applied field E_{appl} , the KAI theory gives the polarization change $\Delta P(t)$ as

$$\frac{\Delta P(t)}{2P_s} = 1 - \exp[-(t/\tau)^n] \quad (1)$$

where n and τ are the effective dimensionality and characteristic time, respectively. τ is inversely proportional to the domain wall velocity. P_s is the spontaneous polarization. This model can be further classified into two cases: the α model, where nucleation takes place with a constant rate during switching; and the β model, where nucleation takes place only at $t = 0$. $n = D + 1$ for the α model, and $n = D$ for the β model, where D is the geometrical dimensionality of the system ($D = 1$ for stripelike domains, $D = 2$ for circular domains and $D = 3$ for spherical domains; see figure 1).

Choosing either the α model or the β model for nucleation is rather arbitrary in the KAI theory.

Although the KAI model has been successfully used to describe the switching kinetics of single-crystalline [7] as well as epitaxial thin-film ferroelectrics [8], it encounters problems when it comes to correctly describing the domain reversal behavior in polycrystalline ferroelectric thin films of high commercial interest, particularly at low applied fields [9–11]. This is understandable because the KAI model assumes an infinite crystal as well as unrestricted domain growth during switching (figure 1). Although these assumptions seem to be acceptable for single-crystalline ferroelectrics, they are highly questionable when we deal with polarization switching in polycrystalline ferroelectrics, for which it is experimentally well known that domain switching in these capacitors is highly restricted by grain boundaries [12] and/or 90° domain walls [13]. The retardation behaviors at low fields in polycrystalline ferroelectric thin films have been tentatively explained through polarization processes with a broad distribution of relaxation times [9], a nucleation-limited-switching (NLS) model [11] or the Lorentzian distribution of logarithmic switching times, very recently [10].

Furthermore, the effect of the depolarization field E_{dep} during polarization switching has been totally ignored in these

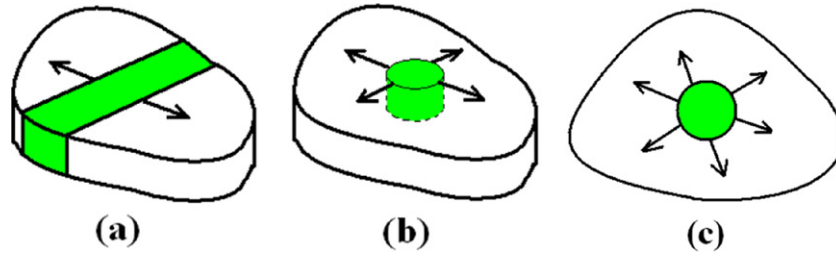


Figure 1. Shapes of reversed domains and their dimensionalities in the KAI theory; (a), (b) and (c) correspond to one-, two- and three-dimensional cases, respectively. The shaded (green) region and the white region denote regions with spontaneous polarization pointing in opposite directions.

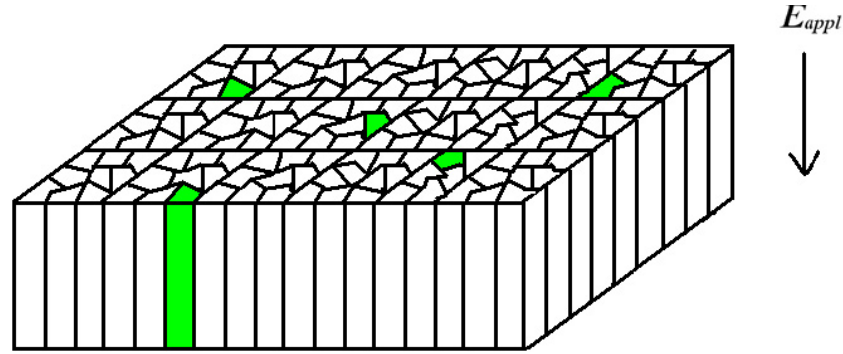


Figure 2. Schematic diagram of the polarization reversal scenario in the present model. The shaded (green) regions denote the switched parts with spontaneous polarization pointing downwards, while the white regions denote the non-switched (or retained) parts with spontaneous polarization pointing upwards. For better illustration, the top/bottom electrodes are not drawn. Not drawn either are the interface passive layers and/or polarization gradient near the electrode and/or finite electrode screening that are believed to induce the depolarization field. Note that the figure is not to scale.

models and scenarios. Although it is a good approximation for bulk ferroelectric materials, it fails for thin-film samples, for which it is apparent that the depolarization effect plays an important role in determining the switching behaviors, especially at medium and low fields.

One can see that a proper theory for describing the switching kinetics of polycrystalline ferroelectrics is still lacking. In this paper, we firstly develop a statistical switching theory for polycrystalline ferroelectrics based on a more realistic nucleation and polarization reversal scenario in these materials. Then the predictions from this model for polycrystalline thin films at low applied fields (where E_{dep} has to be considered) and for polycrystalline thin films at high applied fields or bulk ceramics (where E_{dep} can be neglected) are discussed.

2. A statistical model for switching in polycrystalline ferroelectrics

First of all, let us divide the total area of a polycrystalline ferroelectric capacitor *uniformly* into M_0 parts and assume that under the total field (i.e., the sum of E_{appl} and E_{dep}) polarization switching in this capacitor takes place in a part-by-part or region-by-region manner due to the *blocking* effect of grain boundaries [12], defect planes/dislocations and/or 90° domain walls [13], consistent with the microscopic observations of ferroelectric polycrystalline thin films [12, 14].

In other words, polarization reversal within each part of the film occurs *independently* by formation of an opposite nucleus, followed by relatively quick forward and sideways growth of opposite domains until they reach the boundaries of this part. That is, domain wall motion is only allowed within one part; domain wall motion crossing the boundaries between one part and another is not allowed in our present model (figure 2).

The depolarization field in a poled Pt/PZT/Pt capacitor with interface layers (PZT denotes $\text{Pb}(\text{Zr},\text{Ti})\text{O}_3$) has been written as [15]

$$E_{\text{dep}}(t) = \frac{d_i P(t)}{d \varepsilon_i \varepsilon_0} \quad (2)$$

where d and d_i are the thickness of the film and the interface layer, respectively. ε_i is the interface dielectric constant. $P(t)$ is the time-dependent polarization. Assuming $d = 200$ nm, $d_i = 2$ nm, $\varepsilon_i = 40$ [16] and $P(t) = 30 \mu\text{C cm}^{-2}$, we have $E_{\text{dep}}(t) \sim 85 \text{ kV cm}^{-1}$, which is indeed large enough to play some role during a switching process in ferroelectric thin films, especially at low fields. Note that the depolarization field *unavoidably* appears to some extent in insulating thin-film ferroelectrics due to the poor screening of the bound charge at the interface induced by an interface passive layer and/or polarization gradient near the electrode and/or a finite electrode screening length [17]. In general, it can be written as

$$E_{\text{dep}}(t) = \beta \frac{P(t)}{\varepsilon_f \varepsilon_0} \quad (3)$$

where β is the depolarization factor, ε_f is the ferroelectric dielectric constant. (Note that for mathematical convenience we will use equation (2) rather than equation (3) in the following derivation. Replacing equation (2) by the general form equation (3) or any other specific form for E_{dep} is straightforward.) So, the total field experienced by the film is

$$E_{\text{tot}}(t) = E_{\text{appl}} + E_{\text{dep}}(t) = E_{\text{appl}} + \frac{d_i P(t)}{d\varepsilon_i \varepsilon_0}. \quad (4)$$

It can be seen that the total field is not a constant as assumed in other models, but a time-dependent quantity¹. Let us define the direction of E_{appl} to be positive. Since $E_{\text{dep}}(t)$ is always antiparallel to $P(t)$, $E_{\text{dep}}(t) = \frac{d_i P(t)}{d\varepsilon_i \varepsilon_0} > 0$ (i.e., $E_{\text{dep}}(t)$ is parallel to E_{appl}) at an earlier switching stage, but $E_{\text{dep}}(t) = \frac{d_i P(t)}{d\varepsilon_i \varepsilon_0} < 0$ (i.e., $E_{\text{dep}}(t)$ is antiparallel to E_{appl}) at a later switching stage, depending on whether the total $P(t)$ changes its sign.

Let us begin with a fully poled ferroelectric thin-film capacitor with polarization P_{M_0} at $t = 0 \sim 10^{-13}$ s (the period of an optical phonon) when the poling field is just removed. For simplicity we imagine that the external field E_{appl} is *immediately* applied without the relaxation of P_{M_0} induced by the depolarization field (i.e. the waiting time t_w is slightly larger than 10^{-13} s; see the inset in figure 3). We will return to the situation in which there are noticeable time intervals (and therefore polarization relaxation) between the pulses (i.e., $t_w \gg 10^{-13}$ s) later on. Then we assume $1/\xi(t_N)$ ($\xi \gg 1$) to be the probability that one of the retained parts switches after t_c from the time point where the N th part has *just* switched. t_N is defined as the time interval that the N th part takes to switch. t_c is a characteristic time and can be chosen arbitrarily as long as it ensures that $1/\xi(t_N) \ll 1$ for any t_N , and it disappears later on as we will see. So the probability that one part will not switch after t_c from time t_0 is $[1 - 1/\xi(t_0)]$. Then the probability that one part will survive from switching after t_1 ($t_1 \gg t_c$) from time t_0 is $(1 - \frac{1}{\xi(t_0)})^{t_1/t_c}$. According to the definition of t_N , the total number of the parts that retain their polarization after t_1 (recall that t_1 is the time interval that the *first* part takes to switch) is

$$M_0 - 1 = M_0 \left(1 - \frac{1}{\xi(t_0)}\right)^{t_1/t_c} \quad (5)$$

which can be rearranged into

$$\frac{M_0 - 1}{M_0} = \left(1 - \frac{1}{\xi(t_0)}\right)^{t_1/t_c}. \quad (6)$$

Taking the natural logarithm on both sides of equation (6), we get

$$\begin{aligned} \ln \frac{M_0 - 1}{M_0} &= \frac{t_1}{t_c} \ln \left(1 - \frac{1}{\xi(t_0)}\right) \\ &= \frac{t_1}{t_c} \left[-\frac{1}{\xi(t_0)} - \frac{1}{2} \left(\frac{1}{\xi^2(t_0)}\right) + \dots \right]. \end{aligned} \quad (7)$$

¹ Note that for simplicity we define E_{appl} to be the field applied on the ferroelectric part of the sample in this work; E_{appl} is equal to or slightly less than the external field for some thin-film capacitors containing passive layers, and can be readily calculated.

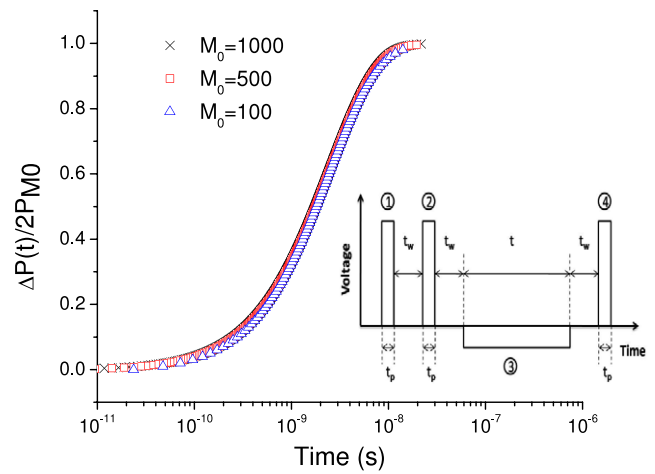


Figure 3. The (Y, X) plots of $(\frac{\Delta P(t)}{2PM_0} = \frac{N}{M_0}, t = \sum_{i=1}^N t_i)$ according to equation (12) for $M_0 = 100, 500$ and 1000 .

Considering that $\xi(t_0) \gg 1$, we can neglect all the higher order terms and have

$$\frac{M_0 - 1}{M_0} = \exp\left(-\frac{t_1}{t_c \xi(t_0)}\right). \quad (8)$$

Recall Merz's law [18]:

$$\frac{1}{t_{\text{sw}}} = \frac{1}{t_{\infty}} \exp\left(-\frac{\alpha}{E_{\text{tot}}}\right) \quad (9)$$

where t_{sw} and t_{∞} are the switching time for E_{tot} and an infinite field, respectively. α is the activation field for switching. According to the meaning of $1/\xi(t_0)$ defined above, we have

$$\frac{1}{\xi(t_0)} = \frac{t_c}{t_{\text{sw}}(t_0)} = \frac{t_c}{t_{\infty}} \exp\left(-\frac{\alpha}{E_{\text{tot}}(t_0)}\right). \quad (10)$$

Inserting equations (4) and (10) into equation (8), we have

$$\frac{M_0 - 1}{M_0} = \exp\left(-\frac{t_1}{t_{\infty}} \exp\left(-\frac{\alpha}{\left(E_{\text{appl}} + \frac{d_i P_{M_0}}{d\varepsilon_i \varepsilon_0}\right)}\right)\right). \quad (11)$$

Similarly, we get a series of *feedback* equations:

$$\begin{aligned} \frac{M_0 - 2}{M_0 - 1} &= \exp\left(-\frac{t_2}{t_{\infty}} \exp\left(-\frac{\alpha}{\left(E_{\text{appl}} + \frac{d_i P_{M_0-1}}{d\varepsilon_i \varepsilon_0}\right)}\right)\right) \\ &\vdots \\ \frac{M_0 - N - 1}{M_0 - N} &= \exp\left(-\frac{t_{N+1}}{t_{\infty}} \exp\left(-\frac{\alpha}{\left(E_{\text{appl}} + \frac{d_i P_{M_0-N}}{d\varepsilon_i \varepsilon_0}\right)}\right)\right) \\ &\vdots \\ \frac{M_0 - M_0}{M_0 - M_0 + 1} &= \frac{0}{1} = \exp\left(-\frac{t_{M_0}}{t_{\infty}} \exp\left(-\frac{\alpha}{\left(E_{\text{appl}} + \frac{d_i P_1}{d\varepsilon_i \varepsilon_0}\right)}\right)\right) \end{aligned} \quad (12)$$

where $N = [0, 1, \dots, (M_0 - 1)]$ and $P_{M_0-N} = \frac{M_0-2N}{M_0} P_{M_0}$. $P_{M_0-N} > 0$ when $N < M_0/2$; $P_{M_0-N} \leq 0$ when $N \geq M_0/2$. Note that equation (12) contains *no* adjustable parameter. t_∞ can be worked out both experimentally and theoretically for a specific sample. Merz obtained $t_\infty = 10$ ns for a BTO single crystal of $20 \mu\text{m}$ (t_∞ decreases as d decreases) [18], in agreement with $t_\infty = 13$ ns achieved by Scott *et al* for submicron PZT films [19]. Notice that the fastest switching time measured so far is 220 ps in a circuit with a small RC constant of ~ 45 ps [20], where t_∞ should be around ~ 100 ps or less. From a theoretical point of view, we could estimate $t_\infty \sim t_{\text{pg}} = d/v$, where t_{pg} is the propagation time of needlelike domains, v is the sound velocity ($\sim 2000 \text{ m s}^{-1}$). For a film with $d = 200$ nm, we get $t_\infty \sim t_{\text{pg}} = 100$ ps. One can see that t_∞ depends very much on the parameters of a specific sample. t_∞ varies from 100 ps to 10 ns for a normal thin-film ferroelectric capacitor; and t_∞ in equations (10)–(12) should be smaller because it is the value for one part of the whole capacitor. For simplicity, we use $t_\infty = 1$ ns in this work.

Note that a switching model for ferroelectric thin films was presented by Chandra *et al* [21], who emphasized the field dependence of the nucleation rate per unit area and showed that it leads to the observed thickness scaling of the coercive field in ferroelectric films over five decades.

Let us make some remarks about our model.

2.1. M_0 effect

The (Y, X) plots of $(\frac{\Delta P(t)}{2P_{M_0}} = \frac{1 - \frac{P_{M_0-N}}{P_{M_0}}}{2} = \frac{N}{M_0}, t = \sum_{i=1}^N t_i)$ have been plotted in figure 3 according to equation (12) for $M_0 = 100, 500$ and 1000 , where we took some typical values for a polycrystalline ferroelectric capacitor: $E_{\text{appl}} = 500 \text{ kV cm}^{-1}$, $P_{M_0} = 30 \mu\text{C cm}^{-2}$, $d = 200$ nm, $\varepsilon_i/d_i = 20 \text{ nm}^{-1}$, $\alpha = 500 \text{ kV cm}^{-1}$ [8, 20, 22, 23], and $t_\infty = 1$ ns as justified above. One can see that the change of M_0 has little effect on the curves in figure 3. The profiles are stabilized when $M_0 \rightarrow \infty$ (e.g. the curve for $M_0 = 500$ essentially overlaps with that for $M_0 = 1000$). In view of the derivation of equation (12) it is obvious that *there is no analytic equation that can describe the whole curve*; each data point has to be calculated using equation (12) and $t = \sum_{i=1}^N t_i$ for given $\frac{\Delta P(t)}{2P_{M_0}} = \frac{N}{M_0}$. From equation (12) one can see that the effect of the change of t_∞ is to just slightly shift the whole curve along the X axis without changing its profile.

2.2. Polycrystalline thin films at low or medium E_{appl}

The (Y, X) plots of $(\frac{\Delta P(t)}{2P_{M_0}} = \frac{N}{M_0}, t = \sum_{i=1}^N t_i)$ have been plotted in figure 4 according to equation (12) for $E_{\text{appl}} = (500, 400, 300, 200, 150, 100, 90, 70, 50, 30, 10, \text{ and } 0) \text{ kV cm}^{-1}$, respectively. From figure 4 we see that the curves shift to the right along the time axis for lower fields. We also see that at low E_{appl} the switching process is highly retarded and expands over many time decades: it covers ~ 3 decades for $E_{\text{appl}} = 500$ and 400 kV cm^{-1} , ~ 4 decades for $E_{\text{appl}} = 300$ and 200 kV cm^{-1} , and ~ 6 decades for $E_{\text{appl}} = 150 \text{ kV cm}^{-1}$; it dramatically increases to ~ 15

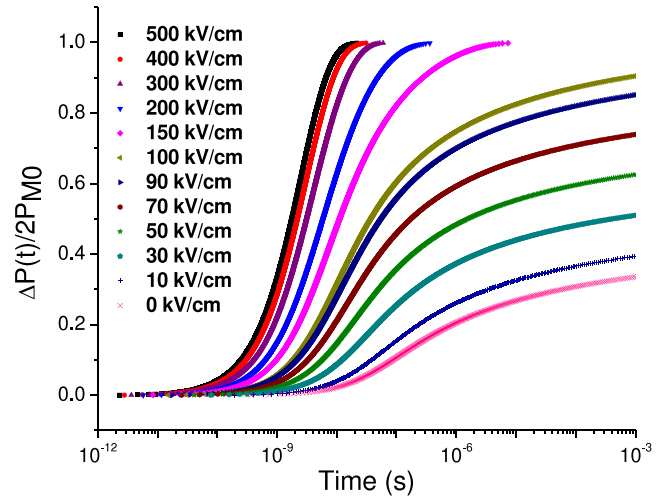


Figure 4. The (Y, X) plots of $(\frac{\Delta P(t)}{2P_{M_0}} = \frac{N}{M_0}, t = \sum_{i=1}^N t_i)$ according to equation (12) ($M_0 = 1000$) for $E_{\text{appl}} = (500, 400, 300, 200, 150, 100, 90, 70, 50, 30, 10, \text{ and } 0) \text{ kV cm}^{-1}$.

decades for $E_{\text{appl}} = 100 \text{ kV cm}^{-1}$ when E_{appl} is comparable with the maximum $E_{\text{dep}} \sim 85 \text{ kV cm}^{-1}$; and the switching time t_{sw} essentially goes to infinity for $E_{\text{appl}} < E_{\text{dep}}^{\text{max}} \sim 85 \text{ kV cm}^{-1}$ (i.e., it can never be fully switched as expected) in our imaginary system. Note that the ‘fan structure’ of the profiles and the retardation behavior at low E_{appl} give at least qualitative explanations of the observations in the literature on polycrystalline thin-film samples: see figure 4 in [9], figure 2 in [11], figure 1 in [10] and figure 2 in [24]. Also note that the $E_{\text{appl}} \sim 0 \text{ kV cm}^{-1}$ case essentially corresponds to the switching curve driven purely by the depolarization field (i.e. the case of retention loss).

Finally, we noticed that the ‘pulse method’ set-ups for switching measurements used by other people were different from the ideal one that we assumed in this work (see the inset in figure 3): we used $t_w \sim 10^{-12}$ s as mentioned before, to avoid the polarization relaxation loss; $t_w \sim 500 \text{ ns} = 5 \times 10^{-7}$ s [10, 24], $t_w \sim 1$ s [11] and 10 s [8] were used in the previous works. It is well known that significant retention loss occurs within 10^{-3} s after the poling pulse is removed [17, 25] (readers can also get some ideas about the magnitude of the polarization loss as a function of time from the curve of $E_{\text{appl}} \sim 0 \text{ kV cm}^{-1}$ in figure 4). Therefore, the real situations in those measurements could be very complex: retention loss driven by pure E_{dep} takes place during time interval t_w between pulse 2 and pulse 3 (inset in figure 3), switching occurs driven by the residual $E_{\text{dep}} + E_{\text{appl}}$ during time interval t of switching pulse 3, and another retention loss in the opposite direction takes place driven by the opposite E_{dep} during the time interval t_w between switching pulse 3 and read pulse 4. So, instead of $2P_s = 2P_{M_0}$ used by this work, the researchers were essentially working on $2P_s = 2P_{M_0-N_R}$, where N_R is the number of relaxed or backswitched parts, and depends on the value of t_w .

The t_w problem mentioned above as well as the *feedback* nature of our model that requires some pre-knowledge about t_∞ , α , P_{M_0} and ε_i/d_i for a specific sample prevent us from giving a further quantitative description of those low E_{appl}

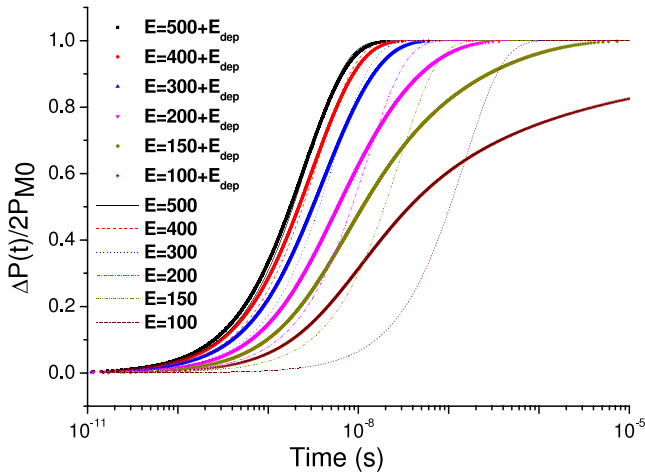


Figure 5. The profiles of $\Delta P(t)/2P_{M_0}$ as a function of t according to equation (15), where $E_{\text{appl}} = (500, 400, 300, 200, 150, \text{ and } 100) \text{ kV cm}^{-1}$. The curves according to equation (12) ($M_0 = 1000$) for these E_{appl} have also been plotted for comparison.

switching data and/or fitting them using software like Origin. Therefore, in this theoretical paper we would rather like to make these predictions and qualitative comparisons with the data in the literature, leaving quantitative confirmation open to future *better* experimental tests. In this sense, we strongly suggest that experimentalists use a t_w that is as short as possible in order to simplify switching studies. However, we will show that in the high E_{appl} limit equation (12) reduces to an *analytic* form. In this case, experimental data fitting does indeed become possible as shown later on.

2.3. Polycrystalline thin films at high E_{appl} and polycrystalline/ceramic bulks

If $E_{\text{appl}} \gg E_{\text{dep}}$ (i.e. E_{dep} can be neglected), according to equation (12) we have

$$t_{N+1} = \frac{-t_\infty \ln\left(\frac{M_0 - N - 1}{M_0 - N}\right)}{\exp\left(-\frac{\alpha}{E_{\text{appl}}}\right)}. \quad (13)$$

So

$$\begin{aligned} t &= \sum_{i=1}^N t_i = \frac{-t_\infty}{\exp\left(-\frac{\alpha}{E_{\text{appl}}}\right)} \\ &\times \left[\ln\left(\frac{M_0 - 1}{M_0}\right) + \dots + \ln\left(\frac{M_0 - N}{M_0 - N + 1}\right) \right] \\ &= \frac{-t_\infty}{\exp\left(-\frac{\alpha}{E_{\text{appl}}}\right)} \ln\left(\frac{M_0 - N}{M_0}\right). \end{aligned} \quad (14)$$

So we have

$$\frac{\Delta P(t)}{2P_{M_0}} = \frac{N}{M_0} = 1 - \exp\left(-\frac{t}{t_\infty} \exp\left(-\frac{\alpha}{E_{\text{appl}}}\right)\right). \quad (15)$$

One can see that equation (15), a simplified version of equation (12) when $E_{\text{appl}} \gg E_{\text{dep}}$, is actually equivalent to

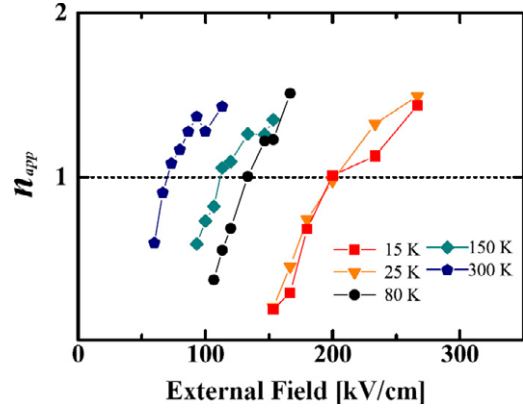


Figure 6. Values of n_{app} as a function of external field for various temperatures (after the work by Jo *et al* [10]).

equation (1) in the KAI model when $n = 1$ and assuming

$$\frac{1}{\tau} = \frac{1}{t_\infty} \exp\left(-\frac{\alpha}{E_{\text{appl}}}\right), \quad (16)$$

i.e. Merz's law. This is remarkable due to the completely different nucleation and polarization reversal scenarios and derivation approaches adopted in developing these two theories [2–4]. Comparing equation (16) with equation (9), we notice that the average switching time t_{sw} for one part is essentially the characteristic time τ for an ensemble of the total M_0 parts at given E_{appl} .

Figure 5 shows the profiles of $\Delta P(t)/2P_{M_0}$ as a function of t according to equation (15), where $E_{\text{appl}} = (500, 400, 300, 200, 150, \text{ and } 100) \text{ kV cm}^{-1}$. For comparison, the curves according to equation (12) for these E_{appl} have also been plotted. One can see that the deviation between the curve according to equation (15) and the one according to equation (12) decreases as E_{appl} increases. At $E_{\text{appl}} = 500 \text{ kV cm}^{-1}$ (where $E_{\text{appl}} \gg E_{\text{dep}}$), they almost overlap with each other, which justifies E_{dep} being neglected, and equation (15) holds for polycrystalline thin films at high fields. At medium or low E_{appl} , however, the effect of E_{dep} is to promote switching at an earlier switching stage and retard it at a later switching stage (figure 5).

Therefore, our model predicts that $n \sim 1$ *ideally* for the switching curve in polycrystalline thin films at high E_{appl} , in good agreement with the data of Jo *et al*, who obtained $n_{\text{app}} = 1 \pm 0.4$ at room temperature (n_{app} denotes ‘apparent’ n), $n_{\text{app}} = 1 \pm 0.4$ at 150 K, $n_{\text{app}} = 1 \pm 0.6$ at 80 K, and $n_{\text{app}} = 0.9 \pm 0.6$ at 25 and 15 K for various fields (figure 6, after the work by Jo *et al* [10]). So n does indeed center at 1. The reason why some ‘apparent’ n values at higher E deviate from the ideal value and are slightly larger than 1 is probably because of the switching promotion effect between adjacent parts [26]. The reason why $n_{\text{app}} < 1$ at low fields [10] is the promotion (or retardation) effect of E_{dep} at the earlier (or later) switching stage discussed above. Actually, an easy way to estimate the n value in the KAI model (equation (1)) is to see how many decades the curves in figure 4 expand over, e.g. one-decade expansion leads to $n_{\text{app}} \sim 3, 1.5$

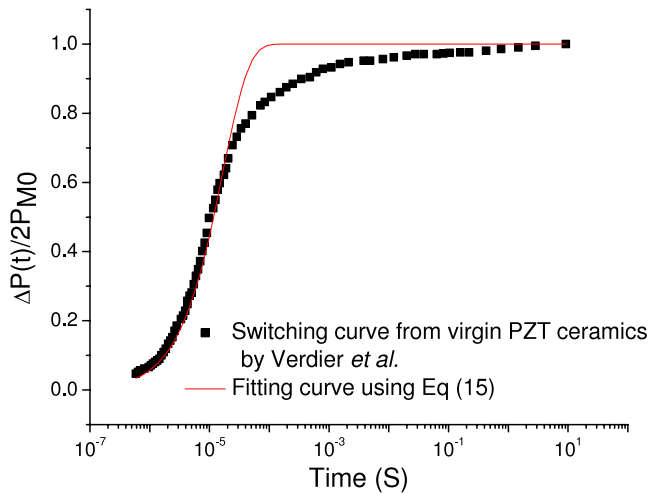


Figure 7. Polarization switching data of Verdier *et al* (the curve for the non-fatigued (NF) sample of figure 1 of [27]) for commercialized PZT bulk ceramics and the curve fitted with equation (15).

decades to $n_{app} \sim 2$, ~ 3 decades to $n_{app} \sim 1$. Expansion over more than four decades always gives rise to $n_{app} < 1$.

Our model (figures 4 and 5) also implies that the KAI model (which completely ignores E_{dep}) cannot give a good description for the data at low E_{appl} . Tentative fitting always gives very poor fitting quality together with $n_{app} < 1$ (see figures 1 and 2 in [10]), and that is why we call it ‘apparent’ n , or n_{app} , here. Note that an n value less than 1 is not physically reasonable according to the KAI model, since the growth dimensionality could never be less than 1 no matter how we mix the α model with the β model.

Finally let us look at the case of ceramic bulks (i.e., $d \gg 100$ nm, the large thickness limit) where E_{dep} goes to zero according to equation (2) and therefore could also be neglected. Polarization switching data of Verdier *et al* (the curve for the non-fatigued (NF) sample in figure 1 of [27]) for commercialized virgin PZT ceramic samples have been fitted using equation (15) in figure 7. One can see that equation (15) having $n \sim 1$ in the ideal case, derived by neglecting E_{dep} , can indeed give a good description for the switching kinetics of polycrystalline/ceramic bulk materials. Best fitting (not shown) gives $n_{app} = 0.90$, close to 1. Again, a weak retardation at a later stage of the switching curve could also be seen due to the depolarization effect inside the material and/or near the electrode. The fitting curve in figure 7 gives $\frac{1}{\tau} = \frac{1}{t_{\infty}} \exp(-\frac{\alpha}{E_{appl}}) = 59\,250.17$. Since $E_{appl} = 20$ kV cm $^{-1}$ [27], we have $t_{\infty} = 6.21 \times 10^{-6}$ s for $\alpha = 20$ kV cm $^{-1}$, $t_{\infty} = 1.39 \times 10^{-6}$ s for $\alpha = 50$ kV cm $^{-1}$, and $t_{\infty} = 1.14 \times 10^{-7}$ s = 114 ns for $\alpha = 100$ kV cm $^{-1}$. For reasonable α values, t_{∞} for ceramic bulks is about 2–4 orders of magnitude higher than those for thin films, which is expected.

Having shown that E_{dep} becomes negligible for ferroelectric thin films at high E_{appl} (i.e., $E_{appl} \gg E_{dep}$) or for bulk ceramics (i.e. $d \gg 100$ nm and E_{dep} goes to zero), we note that E_{dep} also varies with the change of electrodes as well as the ferroelectric material. It has been reported that although an interfacial passive layer forms at the PZT/metal

interface (e.g. PZT/Pt) there is no interface layer observed at PZT/oxide interfaces (e.g. PZT/RuO $_2$, PZT/SrRuO $_3$, etc) and SrBi $_2$ Ta $_2$ O $_9$ (SBT)/metal interfaces (e.g. SBT/Pt) (see [28] and the references therein). Additionally, it is believed that conductive oxide electrodes (e.g. SrRuO $_3$) have a larger screening length (and therefore large field penetration within the electrodes) than metal electrodes such as Pt or Au [29]. As we mentioned above, the magnitude of the depolarization field is very sensitive to the interface passive layer and/or polarization gradient near the electrode and/or the finite electrode screening length of a specific ferroelectric system (see equation (2) or its general form equation (3)). Therefore the switching kinetics of a ferroelectric capacitor will also be affected by the change of electrodes due to the change of E_{dep} according to our model. Our model predicts that the switching time of a polycrystalline ferroelectric capacitor could be tuned via the choice of electrodes for given E_{appl} (figure 5); the minimum switching time (and therefore the fastest switching speed) could be achieved by properly choosing electrodes that cause negligible depolarization field in the sample.

3. Conclusions

In summary, we develop a statistical switching model for polycrystalline ferroelectrics based on more realistic assumptions for nucleation and polarization reversal scenarios. This model is different from both the KAI model and the NLS model. The retardation behavior for polycrystalline thin films at medium or low fields, which cannot be described using the traditional KAI model, can be well explained using this model after incorporating a time-dependent depolarization field. Furthermore, this model predicts $n = 1$ for the *ideal* case for polycrystalline thin-film ferroelectrics at high fields and bulk ceramics, which is in good agreement with the experimental data published previously.

Acknowledgments

I am grateful to the anonymous referee for his/her helpful comments on this paper.

References

- [1] Merz W J 1954 *Phys. Rev.* **95** 690
- [2] Ishibashi Y 1996 *Ferroelectric Thin Films: Synthesis and Basic Properties* ed C P de Araujo, J F Scott and D V Taylor (London: Gordon and Breach) p 135
- [3] Ishibashi Y and Takagi Y 1970 *J. Phys. Soc. Japan* **31** 506
- [4] Orihara H, Hashimoto S and Ishibashi Y 1994 *J. Phys. Soc. Japan* **63** 1031
- [5] Kolmogorov A N 1937 *Izv. Akad. Nauk, Ser. Math.* **3** 355
- [6] Avrami M 1940 *J. Chem. Phys.* **8** 212
- [7] Hashimoto S, Orihara H and Ishibashi Y 1994 *J. Phys. Soc. Japan* **63** 1601
- [8] So Y W *et al* 2005 *Appl. Phys. Lett.* **86** 092905
- [9] Lohse O *et al* 2001 *J. Appl. Phys.* **89** 2332
- [10] Jo J Y *et al* 2007 *Phys. Rev. Lett.* **99** 267602
- [11] Tagantsev A K *et al* 2002 *Phys. Rev. B* **66** 214109
- [12] Stolichnov I *et al* 2005 *Appl. Phys. Lett.* **86** 012902

- [13] Li W and Alexe M 2007 *Appl. Phys. Lett.* **91** 262903
- [14] Hong S *et al* 1999 *J. Appl. Phys.* **86** 607
- [15] Tagantsev A K and Stolichnov I A 1999 *Appl. Phys. Lett.* **74** 1326
- [16] Lou X J *et al* 2007 *Phys. Rev. B* **75** 224104
- [17] Benedetto J M, Moore R A and McLean F B 1994 *J. Appl. Phys.* **75** 460
- [18] Merz W J 1956 *J. Appl. Phys.* **27** 938
- [19] Scott J F *et al* 1988 *J. Appl. Phys.* **64** 787
- [20] Li J *et al* 2004 *Appl. Phys. Lett.* **84** 1174
- [21] Chandra P *et al* 2004 *Ferroelectrics* **313** 7–13
(arXiv:cond-mat/0310074)
- [22] Scott J F 2000 *Ferroelectric Memories* (Berlin: Springer)
- [23] Song T K *et al* 1998 *Appl. Phys. Lett.* **73** 3366
- [24] Jo J Y *et al* 2008 *Appl. Phys. Lett.* **92** 012917
- [25] Jenkins I G *et al* 1998 *Appl. Phys. Lett.* **72** 3300
- [26] Lou X J 2008 at press
- [27] Verdier C *et al* 2004 *Appl. Phys. Lett.* **85** 3211
- [28] Jin H Z and Zhu J 2002 *J. Appl. Phys.* **92** 4594
- [29] Dawber M *et al* 2003 *J. Phys.: Condens. Matter* **15** L393